Pattern Anal Applic (2013) 16:663–678
DOI 10.1007/s10044-012-0287-5

INDUSTRIAL AND COMMERCIAL APPLICATION

Automatic authentication of color laser print-outs using machine identification codes

Joost van Beusekom · Faisal Shafait · Thomas M. Breuel

Received: 12 May 2011 / Accepted: 12 July 2012 / Published online: 9 August 2012

Abstract Authentication of documents can be done by detecting the printing device used to generate the print-out. Many manufacturers of color laser printers and copiers designed their devices in a way to integrate a unique tracking pattern in each print-out. This pattern is used to identify the exact device the print-out originates from. In this paper, we present an important extension of our previous work for (a) detecting the class of printer that was used to generate a print-out, namely automatic methods for (b) comparing two base patterns from two different print-outs to verify if two print-outs come from the same printer and for (c) automatic decoding of the base pattern to extract the serial number and, if available, the time and the date the document was printed. Finally, we present (d) the first public dataset on tracking patterns (also called machine identification codes) containing 1,264 images from 132 different printers. Evaluation on this dataset resulted in accuracies of up to 93.0 % for detecting the printer class. Comparison and decoding of the tracking patterns achieved accuracies of 91.3 and 98.3 %, respectively.

J. van Beusekom (✉) · F. Shafait
German Research Center for Artificial Intelligence (DFKI),
67663 Kaiserslautern, Germany
e-mail: j_v_b@gmx.net

F. Shafait
e-mail: Faisal.Shafait@dfki.de

T. M. Breuel
Image Understanding and Pattern Recognition Group,
Department of Computer Science, University of Kaiserslautern,
67663, Kaiserslautern, Germany
e-mail: tmb@informatik.uni-kl.de

Keywords Machine identification code · Counterfeit protection · Document authentication · Color laser printer identification

1 Introduction and related work

Hails [10] defines authentication in the context of documents as "*showing that writing is what it is claimed to be*". In the context of printed documents, the focus is to make sure that the print-out has been created by the person or company that it claims and that all the contents are genuine.

In every-day life, people heavily rely on the genuineness of documents of many kinds, e.g. insurance companies need to make sure that the invoices they process are genuine and have not been altered; employers have to assure that the doctor's note the employee handed in is original; companies need to make sure that the diplomas that the candidate presents are genuine, etc. While in many cases this authentication is done by *manual* visual inspection, this approach cannot be followed in cases where the volume of documents to be verified is just too high as in the case of automated invoice processing systems.

Authentication is often ensured by various types of signatures; these represent a hard to forge feature that only the creator may have added to the document. It can thus be used to prove the document's originality.

Signatures have always been a critical issue, even in ancient times, where the number of paper documents was limited, compared to their tremendously wide-spread use nowadays. The signet rings from the monarchs that were used to sign the documents in ancient times have nowadays been replaced with all kinds of modern security features. A good overview over signature features for document security

is presented by van Renesse [31]. Several categories of features are distinguished, depending on the effort to detect or verify them. Three different levels of effort, called *level of inspection* are commonly being distinguished:

- *First line inspection:* This groups all the inspection methods that can be done using only the unaided human senses. Examples of signatures that can be used in a first line inspection are watermarks and holograms.
- *Second line inspection:* Inspections requiring additional tools to verify a feature or a document fall into this category. Examples are inks that are only visible under ultra-violet light or bar codes that are only readable using a bar code scanner.
- *Third line inspection:* This category covers the more sophisticated analysis that is normally done by experts, e.g. questioned document examiners. Examples are physical and chemical analysis of the ink composition to date a document.

There is a vast variety of features available to make documents relatively secure even through first line inspection, e.g. using special sort of paper, eventually integrating a watermark, by adding holographic images [26], specialized printing techniques [2] and other physical and chemical signatures [11]. Many other types of features can be found in the literature [30, 32, 33].

Having holograms, bar codes or other extra security features is certainly a reasonable way to make documents more robust against tampering. They require, however, extra steps before or during the creation of a document, which will dramatically increase the costs of producing these. A more practical solution has to be found for assuring the authenticity of documents of every day life without adding extra features.

Therefore, the focus is on using features "inside" the document as a signature, the so-called *intrinsic* features. In contrast to *extrinsic* features that are added only for document security purposes, intrinsic features are byproducts of the normal document generating procedure. This has the advantage that the creators of the documents can continue to use their usual technique to generate the documents while achieving a certain degree of tampering resistance.

Several uses of intrinsic features have been presented in previous publications: printer identification, the process of assigning a print-out to a unique printer or a printer type, has been intensively be studied by different groups. Mikkilineni et al. [1, 13, 14] present features that can used to determine the model of laser printer that was used to print a document.

Choi et al. [8] present an approach for identification of single printers using statistics ass, e.g. skewness, kurtosis and correlation to train a support vector machine (SVM) that is then used to assign a print-out to its originating printer. Results are given on a non-public dataset containing print-outs of only nine different printers.

Schreyer et al. [22–24] worked on detecting the printing technique used to print a document. Also, classification between printed documents and copied versions of printed documents has been analyzed. Using discrete cosine transform (DCT) features, good performance could be shown even when scanning with moderate resolutions of 400 dpi.

Jiang et al. [12] presented an approach also using DCT features to identify the printer model. Multi-size block DCT coefficients are extracted to train an SVM, that is used in a second step for classification. Evaluation results are given on a very small dataset, consisting of six printers only.

Another frequent intrinsic document feature is handwriting. Many printed documents contain handwritten parts as notices or signatures. Two related questions can be distinguished: off-line writer identification and off-line signature verification. In this context, off-line means that only the image of the signature or the handwriting is available, in contrast to online data, where stroke information is also used. The first problem consists in identifying the writer of a document in question using a previously trained model of the writers handwriting [5, 19, 21]. In signature verification the question is whether a signature on a document has been generated by the person claimed by the signature or if someone else forged the signature [7, 17].

The introduction of color laser printers and color copiers has made it very easy even for unskilled people to generate high-quality forgeries. Therefore, manufacturers designed their devices in a way that they print a tracking pattern on every print-out. This tracking pattern, also called counterfeit protection system (CPS) or machine identification code (MIC), is unique for each printer and can thus be used to identify the device that was used to generate the print-out.

The CPS codes consist of small yellow dots (see Fig. 1 for an example) that are invisible for the unaided human eye. These dots form a pattern that is repeated many times on a page with a fixed horizontal and vertical spacing. The exact amount of spacing is manufacturer specific and can be used to identify the latter. This repeating pattern is defined as the *base pattern*. It contains information about the printer that was used to generate the print-out, e.g. the serial number of the device. Each printer generates a different base pattern and for some printers even the date and the time when the print-out was generated is encoded [9].

As these CPS codes have been introduced by purpose by the manufacturers, decoding these codes is also possible if the decoding scheme is known. In general, the procedure that a person with the necessary authorization level has to follow in order to find out the exact printer used for

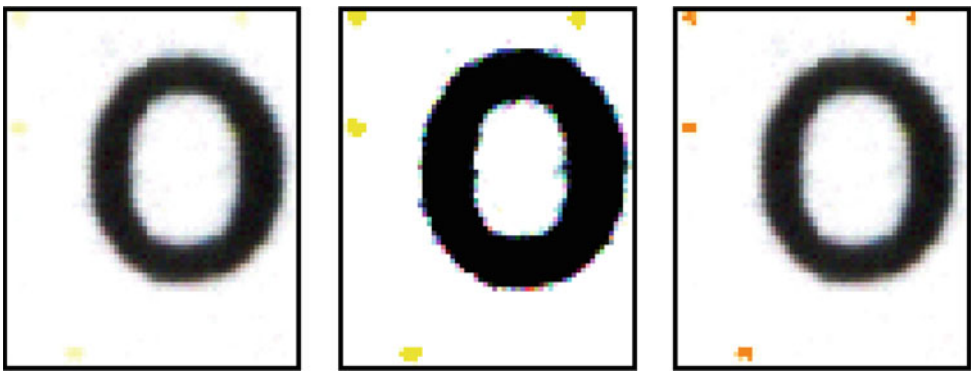

(a) Original **(b)** Adapted curves **(c)** Color exchange

Fig. 1 Examples of CPS dots on a print-out. The *center* and the *right images* have been enhanced to make the dots visible

generating the questioned print-out is the following: the document is send to a licensed laboratory that extracts the so-called *inspection code*. This inspection code can be used by the printer manufacturer to identify the printer that was used and, by comparison to the customer data base, the presumed owner of the printer can be identified.

For privacy reasons, the customer data base is not available for a "public" setup. Furthermore, the information about how to decode the base patterns is classified. In many applications, however, this is not needed; if authentication of a document is needed, e.g. if one needs to make sure that the origin of the document is what the document claims to be, then it may be enough to identify the printer class or to compare the questioned document to a previously known genuine document: if their patterns are identical the questioned document comes from the same device. If they differ, it can be concluded that the document comes from a different source.[1] A modification of this approach can also be used for automatic decoding of the base pattern, which is demonstrated on the Xerox-type patterns for which the decoding scheme is known [9].

In this paper, we considerably extend our previously presented work [28] on (a) detecting the class[2] of printer that was used to generate a print-out by methods for (b) comparing two base patterns from two different print-outs and (c) automatic decoding of the base pattern, if the decoding scheme is known. These extensions are important, because they are needed to use the CPS codes for authenticating documents on a printer level, instead of only on a printer class level. To the authors' best knowledge, this is the first approach to use automatic processing of the CPS codes for identifying the originating printer. The main novelty of both approaches lies in the fact, that by our methods, the CPS codes can be used in a productive setup by everyone for authenticating documents. To the authors' best knowledge, no such method has been published before. Also, the paper presents solutions to solve the comparison and decoding tasks, given the noisy nature of the extracted dots.

Finally, we also present (d) the first public dataset on machine identification codes containing 1,264 images from 132 different printers.

(a) Detection of the manufacturer is done by automating and extending the methodology proposed by Tweedy [27]. By detecting the distance between reoccurring patterns, the so-called horizontal and vertical pattern separating (HPS and VPS) distances can be computed. An approximate assignment to the printer manufacturers can be done on the basis of these two measurements.

(b) By exploiting the redundancy of the repeating base pattern, a method is developed to extract representative candidates of the pattern for comparison to the pattern of a different document. Significant differences in the frequencies of appearing dots can be used to decide if both patterns are identical or not.

(c) Finally, this approach is extended to extract the base pattern which can be used for decoding the pattern, if the decoding scheme is known.

(d) To evaluate the proposed methods, a new dataset has been generated in cooperation with the Electronic Frontier Foundation (EFF). The print-outs collected by the EFF have been scanned and manually ground-truthed resulting in a dataset with 1,264 print-outs from 132 different printers.

The remaining parts of this paper are organized as follows: Sect. 2 describes the extraction of the CPS dots. Printer class identification is described in Sect. 3. Section 4 presents the method for comparison of the CPS codes of two pages. In Sect. 5, the approach for automatic decoding of the CPS base pattern is presented. Details about the

[1] If one source uses more than one color laser printers, the questioned document has to be compared to several base patterns instead of just one.

[2] Roughly speaking, these classes can be assigned to different manufacturers.

newly generated dataset can be found in Sect. 6. Evaluation and results are given in Sects. 7, 7.5 and 7.6. Section 8 concludes the paper.

2 Extraction of the CPS Dots

In a first step, the CPS dots have to be extracted. The dots, also called *yellow* or *tracking* dots are small yellow dots printed on the document. Their size is about 0.007 in. (approximately 4 pixels in a 600 dpi scan). Examples are shown in Figs. 1 and 2.

Several ways are possible to extract the tracking dots: MIT Seeing Yellow [15] proposes to extract the blue channel. Conversion to CYMK and using the Y channel is also possible. A subsequent binarization step [16, 18, 25] could be used to decide between foreground (dot candidate) and background. This approach, however, leads to many false candidates.

Therefore, a manually tuned extraction was chosen; examining the color values of the dots on different pages showed that in RGB color space the R and G values are close to 255, while having a slightly lower B value. The following binarization method was deduced:

$$I(x,y) = \begin{cases} 0 & \text{if } \min(I_R(x,y), I_G(x,y)) - I_B(x,y) < T_1 \\ & \text{and } I_R(x,y) > T_2 \\ & \text{and } I_G(x,y) > T_2 \\ 255 & \text{else} \end{cases} \quad (1)$$

where $I_R(x,y), I_G(x,y)$ and $I_B(x,y)$ are the intensities of the red, green and blue channel of image I at position (x,y), 0 being black and 255 being white. A good choice for the thresholds is $T_1 = 20$ and $T_2 = 240$. These thresholds have been manually set by observing the RGB values of the yellow dots from different documents. The result of this step is a binary image where the black pixels represent dot candidates.

Problems occur if areas with dithered colors are present in the image. After binarization, these areas tend to show significant amounts of pixel noise similar in size to the ones form the CPS code. As these may be very numerous it is preferable to remove these dots to make the system more robust. This filtering is done by morphological closing (dilation followed by erosion) using a quadratic mask. The effect is that dots closer than half of the width of the mask are being connected together, whereas singular dots remain unchanged. A computationally fast implementation using run length encoding for binary morphology was used [6]. The width of the mask is fixed to half of the median distance between the neighboring connected components, which is normally about 12 px.

From the resulting image, the connected components are extracted and filtered: big connected components (width or height bigger than 4 px) are being ignored. This also removes the dithered parts of the image, as these remain connected after the filtering.

Example images in Fig. 3 show the intermediate results for each step. It should be noted that the resulting set of dots is not perfect, in the sense that there may be noise dots and that dots might also be missing due to the following two reasons:

- Overprinted dots: CPS dots are frequently overprinted by text or other document content portions. This leads to a significant number of dots that are not detectable and thus leads to an overall incomplete pattern.
- Noise dots: Some extracted dots may not represent CPS dots. These come from binarization, page contents in yellow color and noisy print-outs due to, e.g. old drums.
- Base pattern ambiguity: Extracting a unique base pattern is less trivial than it may seem; the separating distances do not give any information about where the base pattern starts and ends, thus leading to ambiguities when extracting a base pattern. Moreover, the exact size of the base pattern is unknown. An example for this ambiguity is shown in Fig. 7.

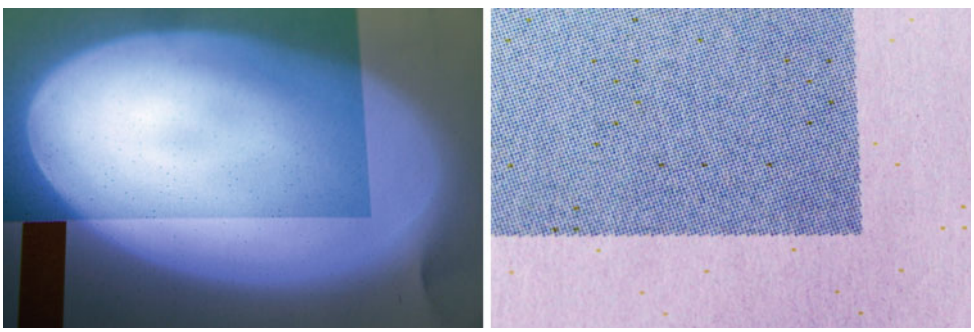

(a) **(b)**

Fig. 2 Examples of CPS dots on a print-out. The *left picture* shows the dots by making them visible using a blue LED light source. The *right image* shows a detail of a high resolution image taken from a part of the page. From the visual appearance of this pattern, it is likely that an HP color LaserJet was used to print this document [27]

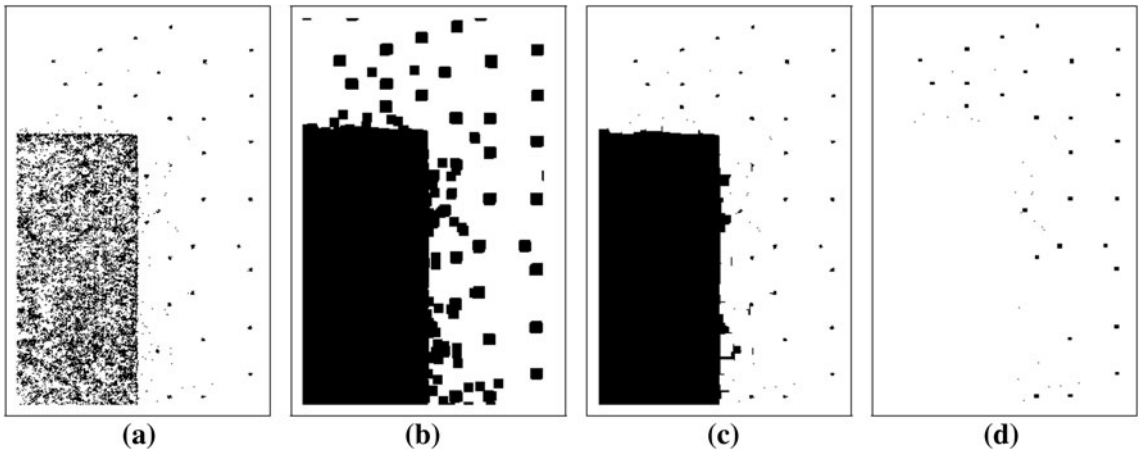

Fig. 3 Visualization of the CPS dot extraction. **a** Binarized image using the task-specific binarization. After dilation image **b** is obtained. Erosion of **b** leads to **c**. Finally, using connected component-based filtering the final image **d** is obtained

This will lead to increased requirements concerning the robustness for the analysis steps.

3 Printer class identification

The proposed method for printer class identification uses the vertical pattern separating distances feature and a classification scheme proposed by Tweedy [27]. This idea is extended to use also the horizontal pattern separation (HPS) distance to cope with the problem that depending on the paper feed inside the printer, the CPS codes may be rotated by 90°.

3.1 Computation of horizontal and vertical pattern separation distances

For reading simplicity, in the following, only the computation of the HPS distance is discussed. The VPS distance follows an analogous scheme, just switching the directions x (horizontal) and y (vertical).

The approach for computing the HPS takes a random local subset of the tracking dots and matches this subset to the remaining dots at approximately the same y position. For each obtained match the translation parameter is t_x. As random selection of a local subset may lead to noise patterns being matched, the whole process is run several times. Statistics on all the obtained translation parameter values are used to estimate the HPS and VPS distance of a pattern. A visualization of the main idea is given in Fig. 4.

The reason for only considering matches on approximately the same y position lies in the fact that not all CPS pattern repetitions are on a regular grid. Some CPS codes repeat their *base pattern* shifted in x direction in neighboring columns. A base pattern is defined as the smallest set of dots that cannot be split into equal sub-patterns and that explains all the tracking dots in the image by just translating it in x and y directions. An example of such a

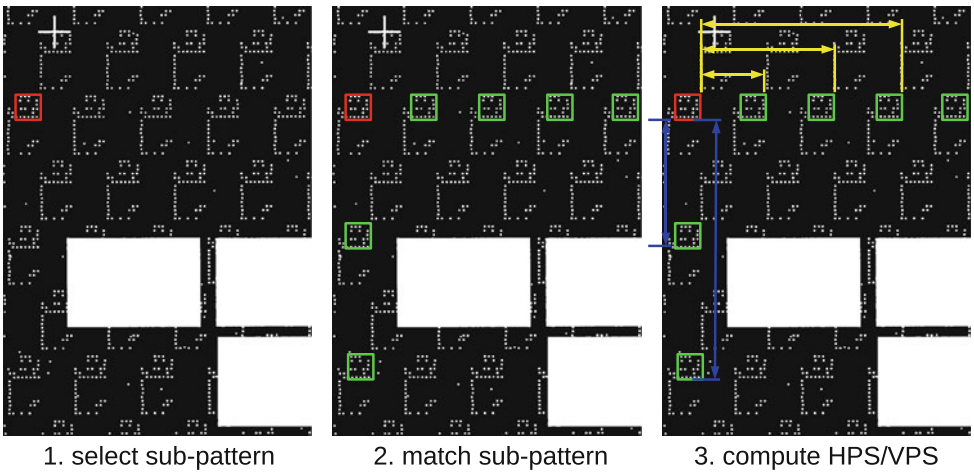

Fig. 4 Computation of HPS and VPS distances: first, a sub-pattern is selected. This is matched at different positions in the same column or row, respectively. The computed translation parameters in x and y direction are used to extract the HPS and VPS distance of the pattern

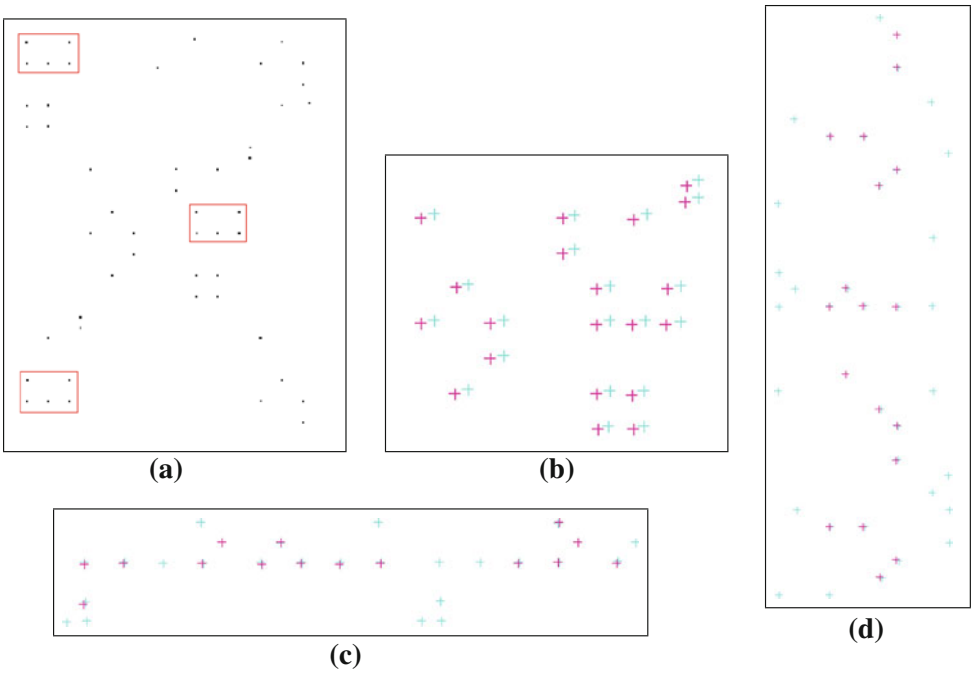

Fig. 5 Example of different patterns. **c**, **d** An example of a horizontal and a vertical search pattern. **a** An example of a non-aligned pattern. **b** The result of the matching: the *blue crosses* represent the sub-pattern to be searched for, the *red ones* represent the repeating patterns above or below the subset pattern. The alignment has been slightly displaced in order to be able to see the *different crosses* (color figure online)

repetitive pattern with offset is shown in Fig. 5a. Without this restriction, the matching would return distances that represent only a fraction of the real distance.

Small variations of t_y have to be allowed to cope with small skew angles α of the document page. Since $\alpha = \operatorname{atan}\frac{t_y}{t_x}$, it becomes clear that the method cannot work, if the skew angle becomes to high, relative to t_x, which is a priori unknown. Therefore, t_y is allowed to vary only little, $\pm 0.75 \times \theta$, where θ is the median distance between closest neighboring point.

The local pattern subset has to be chosen carefully; it must be assured that its width is not bigger than the smallest known HPS distance. Elsewise, only multiples of the distance will be found. Another constraint is that the pattern should be big enough to allow for robust matches. If only a few (e.g. two or three) dots are to be matched, many matches on random positions will be found. Therefore, for each direction a different search pattern is used; starting from a randomly selected dot, an area around this dot is defined such that in the direction of measurement its size is smaller than the smallest known pattern separation distance (currently 0.16 in.). In the other direction, it is extended to a wider area to cover more points. This allows the method to find more robust matches. A visualization of such search patterns is given in Fig. 5c, d.

3.2 Matching the search pattern

After choosing the search patterns, the positions where the dot pattern in the same geometric relation can be found have to be computed. This is done using the technique described by Breuel [3]. It uses an optimal branch-and-bound search algorithm, called RAST (Recognition by Adaptive Subdivision of Transformation Space). This method allows robust and accurate finding of the positions of repetitions of the search patterns. For completeness, a short overview of the algorithm is given here.

RAST optimizes a quality function that is defined as the number of model points (dots from the search pattern) matching an image point (remaining dots) under the error bound ϵ. The RAST algorithm uses a branch-and-bound search for quickly finding a global optimum for the given quality function. The method uses a priority queue containing parameter subspaces ordered by their upper bound quality. The highest upper bound quality subspace is divided into two new subspaces, by splitting it into two parts of equal size. For each part, the new upper bound quality is determined and both subspaces are added into the priority queue. These steps are repeated until a stopping criterion is met.

The RAST algorithm performs a branch-and-bound search on the parameter space (also called transformation space). As for each direction, a separate search is done, the transformation space can thus be reduced to parameter $t_x \in [-W, W]$ for the HPS distance (in the case of the VPS distance: $t_y \in [-H, H]$), where W and H are the page width and height and t_x is the translation parameter in x direction. To be more robust against small distortions of the page when matching in horizontal direction, t_y is set to allow for small variations, too. Examples of the matching results can be found in Fig. 5b.

3.3 Estimating HPS and VPS distances

The HPS and VPS distances are measured using recurring translation values; if a pattern has a certain HPS distance, the translation values returned by the search are most likely multiples of the HPS distance, apart from a few "noise" matches. Using several iterations of the search, a histogram of translation values is generated that shows characteristic peaks having a distance approximately equal to the HPS distance.

As the selection of the search pattern is a random process, the selected search pattern may not represent any pattern but, e.g. only noise dots. It may also happen that a search pattern is chosen that is repeated inside the base pattern. Therefore, several iterations of search pattern selection and matching are run, each returning a set of matching parameters. All these results are collected in one priority queue $R = \{(t_{x,1}, q_1) \ldots (t_{x,n}, q_n)\}$, where q_i is the quality of the match i and n is the total number of results returned by all iterations. The quality q_i is the number of dots from the search pattern that could be matched to the remaining dots. This quality is used to select the best m matches for generating the statistics, as matches with higher quality lead to a higher degree of robustness.

A histogram of the translation values t_x of the m best results is generated by computing all pairwise distances. An example of such a histogram is shown in Fig. 6. From this, the HPS distance is computed by histogram comparison; for all possible HPS distances, a reference histogram is generated. It is generated by distributing equally high peaks in the histograms at all different distances for HPS. All the reference histograms are compared with the measured histogram using Jenson–Shannon–Divergence (JSD) [20]. The reference histogram with the smallest JSD gives us the HPS distance.

4 Comparison of CPS Patterns

After extracting the CPS dots of both pages for which the CPS patterns will be compared, a robust method of comparison of these patterns has to be defined, since the set of extracted dots is not perfect (see Sect. 2).

The straightforward comparison of both sets of points is difficult, since the set of dots on both pages largely depends on the document's content. To avoid this problem, an indirect approach of comparison is chosen; the redundancy of the base pattern is used to generate a prototype pattern model that not only contains the dots on their positions but also their frequencies of appearance (Fig. 7).

The idea is that noise points are randomly distributed and will be present in very different positions throughout all the repetitions of the base pattern. The dots belonging to the pattern, however, will be present at always the same position of the base pattern. By this, an implicit distinction between dots belonging to the pattern and noise dots can be done; if the two extracted prototypes significantly differ in one dot, e.g. a dot being very frequent in the first prototype pattern but being very rare in the second prototype pattern,

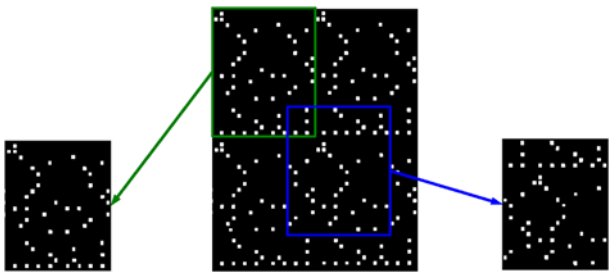

Fig. 7 Example demonstrating the prototype ambiguity: from the dot image in the center, several possible prototypes might be extracted if the start and end points are not known

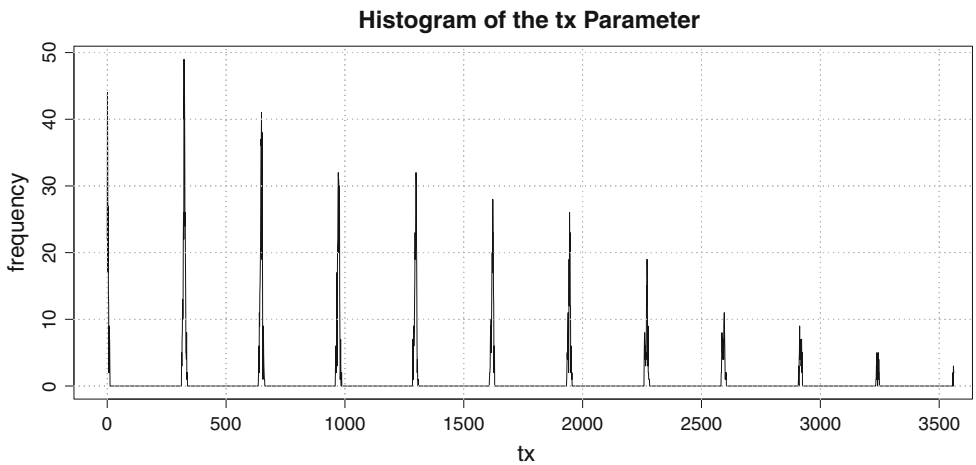

Fig. 6 Histogram of the values of the parameters t_x. One can observe the peaks with the constant distance that is equal to the HPS distance in pixel

the two patterns are considered to be different. The next section explains how the prototype model is computed. Section 4.2 explains how the comparison of two prototype patterns is done.

4.1 Computation of the prototype pattern model

Determining the prototype model is done using the redundancy of the base pattern inside the page. The first step consists of computing the approximate size of the base pattern. This can be done using an approach presented in Sect. 3. Using the HPS and VPS values as an approximate size of the base pattern, a *prototype pattern* is extracted at a random position on the page. This pattern contains all dots inside the window of width VPS and height HPS around a randomly selected dot.

To get a robust prototype pattern, the initial one is used as a model that is matched on the remaining dots of the page. Again, RAST [4] is used for this step in the following way:

```
00 randomly select prototype pattern S
01 match S to the remaining dots
02 for each of the 10% best matches:
03     compute target area of matched prototype
04     for each point p in target area:
05         select the closest point c from the prototype pattern
06         if d(c, p) < D: // Manh. distance
07             increase frequency count for p
08         else:
09             add p to prototype pattern
10 Repeat for I iterations from line 01 on
```

In line 09, the dot p from the target area is added to the search pattern, if the distance is higher than a predefined threshold (normally set to few pixels). This step is necessary to add dots that could belong to the prototype pattern but that were not present in the first, randomly selected prototype set. If these points would not be added, a missing dot in the initial prototype pattern could not be compensated.

The approach is robust to an initially bad choice of the prototype pattern; as the noise dots are randomly distributed on the page, even a noisy prototype pattern is likely to be matched to genuine CPS dots. This will continuously increase the quality of the prototype pattern. Examples of two prototype patterns can be seen in Fig. 9.

4.2 Prototype comparison

Due to the afore-mentioned ambiguity of the base pattern, comparing two prototype patterns from two images directly is not a trivial task (Fig. 8).

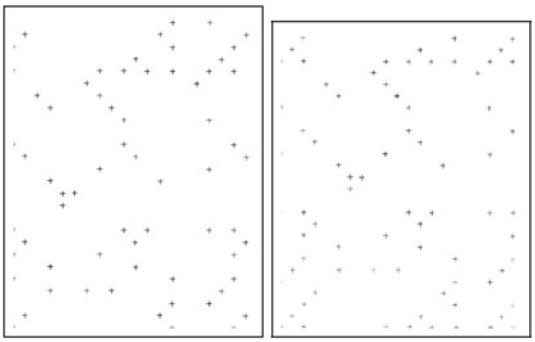

Fig. 8 Examples of extracted prototypes. The darker the *cross*, the higher is its frequency of occurring in a match

To overcome this problem, the prototype from one image is matched to all the dots of the other image. For each dot from the prototype model the frequencies with which they can be matched to the dots of the second image are computed. If a dot is frequently present in the prototype model, it should also be frequent in the other image. If not, both patterns differ. If noise dots are present in the prototype pattern, they will have a low frequency. After matching the prototype to the second image, noise dots should still have a low frequency.

A threshold has to be fixed defining what differences are considered as significant. Consider a normal CPS pattern on a standard page, it should be easily possible to find multiple occurrences of the pattern on that page. One or the other dot might be missing but it is unlikely that by chance always the same dot is missing. On the other side, if noise dots appear, it is unlikely that they will appear in the same position for different repetitions of the base pattern. Therefore, the threshold is set to a high value; infrequent noise will be discarded and for the relevant pattern dots, minor variations in frequency will not influence the outcome. A pattern is defined as different if there is at least one significant difference.

In order to make sure that the second page does not contain any frequent dots that are not present in the first prototype pattern, the comparison has to be done in both ways. Two pages are considered to be different if at least one significant difference in dot frequencies can be found. The threshold defining a significant difference is set to 0.9.

5 Extracting and decoding the Xerox-type base pattern

Some color laser printers and copiers produce CPS patterns that also encode the date and the time a print-out was generated into the pattern. In this case the CPS pattern of two print-outs from the same printer will differ, which will result in a wrong output of the CPS comparison step.

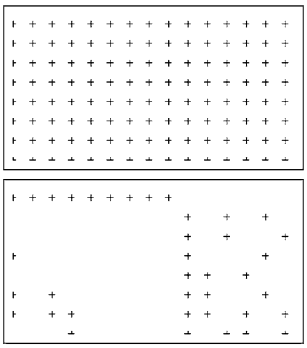

Fig. 9 Examples of the fully occupied and the extracted Xerox-type base patterns

In this part, we present a solution to this problem; we use the previously presented approach to extract the base pattern. This base pattern is then decoded and the comparison can be done on the level of the decoded string. As currently only the decoding for the Xerox DocuLaser is publicly available and as this seems to be the only printer type encoding the time and the date, we explain the method for the application on Xerox-type CPS patterns.

The extraction of the base pattern follows the same approach as the extraction of the prototype model. The sole difference lies in the selection of the initialized search pattern; instead of taking a randomly positioned pattern, a fully occupied base pattern for the CPS pattern type is used. This is a pattern where each crossing on the regular grid of the Xerox pattern is occupied by a dot. An example of a fully occupied Xerox pattern can be found in Fig. 9.

After the prototype matching each point is associated with a certain frequency. Based on this frequency it is decided whether to set each dot as either *on* or *off*. The threshold for this operation can be set at a relatively low level. Without any tuning, 0.1 showed to give suitable results. An example of the fully occupied and an extracted base pattern can be found in Fig. 9.

The decoding of the pattern is done by applying the scheme presented by the EFF [9].

6 The machine code identification dataset

No public dataset was available for testing the proposed method. In cooperation with the EFF, the first public dataset for evaluating methods analyzing CPS codes was generated[3]; in an attempt to gain more information about the CPS codes, the EFF invited the visitors of their web site to send print-outs of the provided test documents, together with additional information as, e.g. the manufacturer, the printer model and its serial number. Those documents were scanned and manually ground-truthed. The scanner used for this task is a Fujitsu *fi-4120C2* automatic document feeding scanner with a maximum optical scanning resolution of 600 dpi and a color depth of 24 bit. All documents were scanned using 600 dpi in full color mode.

A set of 132 sets of test print-outs has been scanned. Each set consists of 8 pages[4] from the EFF printer test set sheets.[5] An example of such a sample set of eight images is given in Fig. 10. On a set level, the ground truth has been generated manually using the information that was handed in on the cover sheet or by supplemental print-outs of, e.g. configuration pages of the printer. The ground truth contains the following information:

- manufacturer of the printer/copier,
- serial number of the printer/copier used to generate the print-outs,
- presence or absence of dots,
- manually measured HPS distance,
- manually measured vertical pattern separation distance,
- vertical pattern separation distance according to the classification given in the paper by Tweedy [27] and
- miscellaneous information.

7 Evaluation and results

Different evaluation procedures have been used to measure the performance of the different approaches presented in this paper. All methods use the previously introduced dataset. Detailed information about the evaluation setups for the different methods are given in the following sections.

Despite the existence of related methods in the area, a comparative analysis could not be done, since none of the datasets used by other researchers has been made public. Furthermore, most of these datasets only contained very few samples from few printers.

7.1 Evaluation of CPS code classification

For the evaluation of the classification based on the HPS and VPS distances, the different classes have to be defined: Tweedy [27] proposed 13 different classes of VPS distances. For the 0.32 and 0.64 in. distances, Tweedy distinguished two different subclasses based on different

[3] The dataset can be downloaded from https://madm.dfki.de/downloads-ds-mic.

[4] Some sets are not complete, others have extra pages, e.g. printer configuration pages.

[5] http://www.eff.org/wp/investigating-machine-identification-code-technology-color-laser-printers#testsheets.

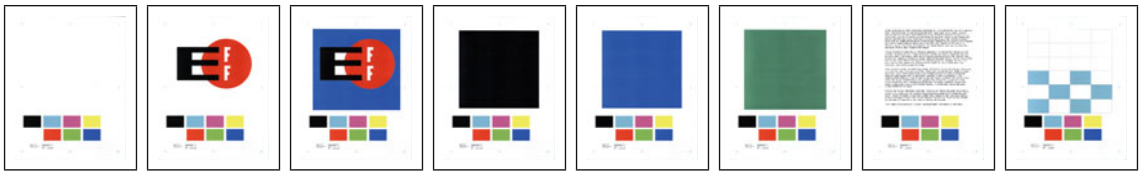

(a) Sh. 0 **(b)** Sh. 1 **(c)** Sh. 2 **(d)** Sh. 3 **(e)** Sh. 4 **(f)** Sh. 5 **(g)** Sh. 6 **(h)** Sh. 7

Fig. 10 Test sheets from the Electronic Frontier Foundation

Fig. 11 Excerpt of the list of printer classes in the evaluation dataset. The HPS and VPS class is given at the *top*, followed by the printers in this class. An other list of printers can be found in [27]

```
0.48 0.96
        Epson Aculaser C1900
        Epson AcuLaser C900
        Epson AcuLaser C1500
        Konica Minolta Magiccolor 2300 DL
        Minolta QMS Magicolor 2210
        Minolta QMS Magicolor 2300DL
        Konica Minolta Magicolor 2300 DL
        ...
0.54 0.69
        HP Color Laserjet 3700DN
        HP Color LaserJet 4700
        HP Color LaserJet 3700DN
        HP Color LaserJet 2840
        HP Color LaserJet 2600N
        HP Color LaserJet 2605DN
        HP Color LaserJet 4600
        ....
0.69 0.54
        Lexmark C910
        Lexmark C912
        Kyocera C2630D
        HP Color LaserJet 5500
        HP Color LaserJet 5500DTN
0.64 1.28
        Epson Aculaser C1100
        Epson Aculaser C3000
        Dell 3110CN
        Dell 5100CN
        Xerox Docucolor 1632
1.28 0.64
        Xerox Phaser 790
        Xerox DocuColor 6060
        Xerox DocuColor 2045
        Xerox DocuColor 12
0.96 0.48
        Minolta  DialtaColor CF 2001
        Minolta-QMS Magicolor 7300
        Konica Bizhub C252
        Konica Minolta Bizhub 350C
-1 -1
        Xerox Phaser 8400N
        Xerox Tektronix Phaser 7750DN
        OKI C9200 Model N31061A
        Samsung CLP-500/XAA
        Brother HL-2700 CN
        OKI C5150n
```

visual characteristics. As these subclasses have the same VPS distance, these are merged into the same class for the current experiments. Thus, 11 different classes are considered: no CPS pattern, 0.16, 0.32, 0.48, 0.50, 0.54, 0.64, 0.69, 0.96, 1.20 and 1.28 in. distances. A list of printers corresponding to the different VPS distances is given in [27]. A list of HPS and VPS pairs and the associated printers can be found in Fig. 11.

As two different measures are computed per page, three different accuracy rates are being computed: the accuracy of computing the correct HPS distance, the accuracy of computing the correct VPS distance and the accuracy of correctly computing both VPS and HPS distances. A list of the different pairs of HPS and VPS distances with more than five occurrences is presented in Table 1. In total, 19 different pairs could be identified in the dataset.

Sheet 6 (Fig. 10g) of each sample contains the most realistic document type for the proposed scenario, namely a page containing mainly text regions. As not all samples are complete, in total 128 images have been used.

The computation of the HPS and VPS distances is done using the method described in Sect. 3. The classification is done using a simple threshold; if the difference between the ground truth distance and the computed distance is less than 0.02 in., it is considered to be in the same class. If no tracking dots are present, no reasonable matches for the search patterns can be found. The document is then considered to be CPS code free.

To test the effect of lower resolutions, the tests have been run in different resolutions of 600 (original resolution), 400, 300 and 200 dpi. The lower resolutions have been obtained by downscaling the images.

As the documents in the dataset were not deskewed after scanning, some show considerable amounts of skew leading to possibly wrong measurements of the HPS and VPS distances. Therefore, the tests have been run on the original images as well as on the deskewed images. A previously published automatic deskewing method [29] has been used to generate the deskewed images.

7.2 Evaluation of CPS code comparison

The test setup for the evaluation of the CPS code comparison is as follows: a set of image pairs was defined to compare print-outs with same HPS and VPS distances. For each sample set, Sheet 3 was compared with Sheet 6 and Sheet 6 was compared with Sheet 3 of the numerically next sample set. If Sheet 3 is not present for a sample set, the

Table 1 List of pairs of HPS and VPS distances occurring more than five times in the dataset

HPS (in.)	VPS (in.)	No. of occurrences
0.54	0.69	34
−1.00	−1.00	31
0.48	0.96	17
0.69	0.54	11
0.64	1.28	7
1.28	0.64	7
0.96	0.48	6

Documents without dots are represented with the pair (−1.0, −1.0). A −1.0 in any other row means that during ground truth generation, the respective HPS or VPS distance was not measurable due to a sparse pattern (see Fig. 13 for examples of sparse patterns)

next Sheet in numerical ascending order is taken (Sheet 4, etc.). By this method a set of 184 comparisons was generated. The ground truth HPS and VPS distances were given as input.

However, as some Xerox printers encode time-variable information into the CPS codes, the comparisons of Xerox print-outs from the same printer have been manually analyzed to see if the patterns vary over time. If this is the case, the expected outcome has been changed to "different", although the patterns come from the same printer.

The evaluation measure is the number of correctly computed outcomes of the comparison. The threshold which decides if a dot significantly differs from one pattern to the other is set to 0.9.

7.3 Evaluation of CPS pattern decoding

For testing the decoding method for the Xerox-type CPS pattern, all the test sheets including the cover page (if available), from samples with Xerox-like patterns were used. Extra sheets have been ignored as some contain black-and-white only print-outs. The extracted information was compared to the ground truth information. If the ground truth information reflected parts of the decoded information, and the decoded information is consistent, the decoding is considered to be correct. This, in most cases, is expressed by parts of the serial number that could be extracted from the CPS pattern. As this criterion of success is a fuzzy one, the extracted information and the relevant ground truth information for each file is given in Sect. 7.6 in order to show the success of the method.

7.4 Results for CPS code classification

The results for the accuracy of the CPS code classification on the original images for the different resolutions can be found in Table 2 and the results on the deskewed images in Table 3.

Table 2 Accuracies for the CPS code classification on the original (skewed) images for different resolutions

(dpi)	HPS corr. (%)	VPS corr. (%)	HPS and VPS corr. (%)
600	87.5	89.1	82.8
400	82.8	78.1	75.0
300	80.5	73.4	72.6
200	71.1	65.6	63.3

At 600 dpi good accuracies can be obtained, especially for the VPS distance measurement

Table 3 Accuracies for the CPS code classification on the deskewed images for different resolutions

(dpi)	HPS corr. (%)	VPS corr. (%)	HPS and VPS corr. (%)
600	90.6	93.0	88.3
400	85.9	78.9	77.3
300	82.8	75.0	75.0
200	74.2	67.2	66.4

At 600 dpi good accuracies can be obtained, especially for the VPS distance measurement

First of all, it can be seen that the accuracies decrease with the resolution. This is not surprising as more and more dots will be missed, the smaller the resolution will be.

Second, it can be noted that the accuracies on the deskewed images are higher than on the skewed ones. Due to the slight rotation, the distances between repeating patterns will be slightly increased but also the matching of the search pattern will return less results leading to a less robust estimation of the HPS and VPS distances. From this, we can conclude that the skew angle decreases the performance of the method. This problem, however, would be rare in real world high-volume scanning scenarios, since deskewing is in most cases a part of the processing pipeline.

The reasons for error can be divided into the following categories:

- *Diffuse patterns:* Some patterns (generated mostly by Canon machines) have an irregular appearance that shows a clearly distinguishable VPS distance but a much less clearer HPS distance. For these patterns, repetitions in horizontal direction are slightly shifted from one repetition to the next. An exact horizontal repetition was not detectable. But due to the error margin given for the matching, it will find a HPS distance that is actually not the correct one when sticking to the definition. This is mostly observed for the 0.16 and 0.32 in. patterns. An example can be found in Fig. 12.

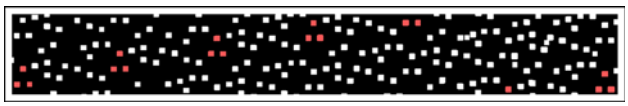

Fig. 12 Example of a diffuse pattern. It can be seen that the pattern is repeating in horizontal direction but that the repetitions have a small offset. A characteristic set of dots is colored in *red* to make the repetitions more easily detectable (color figure online)

- *Bad print quality:* A few documents present printing defects that can be observed when using an old drum or when the paper path of the printer is dirty; this leads to toner spreading all over the page, resulting in many small dots everywhere that cannot be easily distinguished from the CPS dots.
- **Sparse patterns:** On several print-outs the pattern only appears around printed areas. Thus, the large white areas where the dots are easily identifiable do not contain any dots. This significantly reduces the number of dots for reliable matching, leading to mis-detection.

In only few cases, neither the VPS nor the HPS distance could be correctly extracted. In all other cases at least one of the distances was correctly computed, while the other distance was returned either as "no dots present" or as a distance that does not fit any of the classes and that can thus be easily intercepted.

The problem of diffuse patterns could be solved by accurately deskewing the scanned image before processing and reducing the allowed variation during horizontal matching of the search pattern. This would lead to a more accurate estimation of the HPS distance. Another approach would imply verifying if the diffuse patterns appear only in combination with the 0.16 and 0.32 in. VPS distances. In these cases, the HPS distance information could be discarded for printer class detection.

Sparse patterns represent the main problem; depending on the document content, e.g. in case of text, there may be enough dots left to detect a repetitive pattern. For some sample sets, the ground truth had even to be updated as the automatic method correctly found a pattern that had not been detected while manually generating the ground truth. In most cases, however, there are only very few dots left which make it hard for an automated method to detect a recurring pattern. During manual ground truth generation, knowledge about the printer type often helped in steering the search for the HPS and VPS distances into the right direction. Unfortunately, this information is not available in a real world scenario. Concerning the bad print quality, a more sophisticated document cleaning could help.

7.5 Results for CPS code comparison

The results for the evaluation of the accuracy of the CPS code comparison can be found in Table 4. For the test on the 600 dpi images 168 correct decisions and 16 wrong decisions were returned, thus an accuracy of 91.3.

Table 4 Accuracies for the CPS code comparison for different resolutions

(dpi)	Correct	Error	Accuracy (%)
600	168	16	91.3
400	160	24	86.9
300	151	33	82.1
200	112	72	60.9

At 600 dpi good accuracies can be obtained, whereas for 200 dpi results are only slightly better than guessing

A detailed analysis of the errors in the case of the 600 dpi scans showed again that the main issue are *sparse patterns*: for these patterns the dots seem only to be present around page content areas, so not in large white spaces. As only few dots are present and this mostly in areas where dots may be missing due to overlaid text, it is hard to compute a good prototype estimate. Examples of sparse patterns can be seen in Fig. 13.

The problem of the sparse patterns is hard to solve; if only few dots are present, no stable prototype pattern can be generated. In this case the system could try to extract the prototype patterns and display these to an operator who could then decide if the document should be analyzed further. Only comparing the HPS and VPS distance could also be done, as the HPS and VPS distance computation is slightly less sensitive to sparse dot patterns.

A few errors are due to variations in the skew angle of the pages. This can be overcome by initially deskewing the page. As the image 0005 does not contain many text-lines, automatic and accurate deskewing as for the CPS code classification was not possible.

7.6 Results for decoding the Xerox-type pattern

Table 5 contains the list of the images that have been decoded together with the decoded information and the ground truth. It can be seen that from the 129 images that were decoded, 119 were correctly or at least consistently decoded. Sample set 0041 could not be decoded correctly due to sparse patterns. Discarding this sample set from the accuracy measurement, only two errors were made in the decoding, leading to an accuracy of 98.3 % (119 out of 121 remaining patterns were correctly decoded) (Fig. 14).

One issue is related to the threshold defining when a dot is considered *on* or *off*. The default value of 0.5 showed to lead in rare cases to dots that are falsely set to *on*. This problem could be solved by more carefully choosing the threshold. One could also use a more sophisticated method

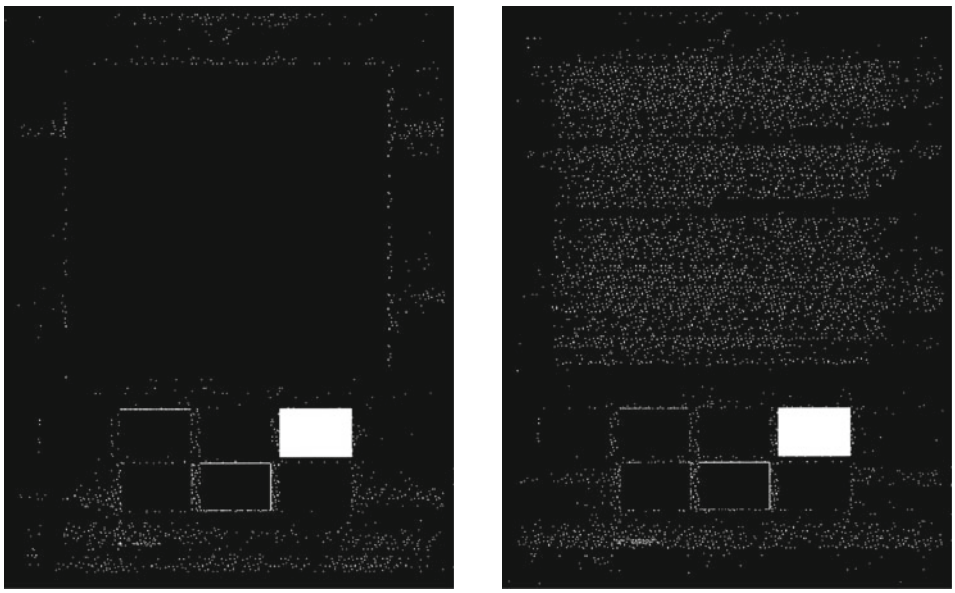

Fig. 13 Example of sparse patterns. It should be noticed that for **a** Sheet 0057-0004 only very few dots are present. For the image **b** 0057-0006 containing Sheet 6, more dots can be observed, especially in the text area

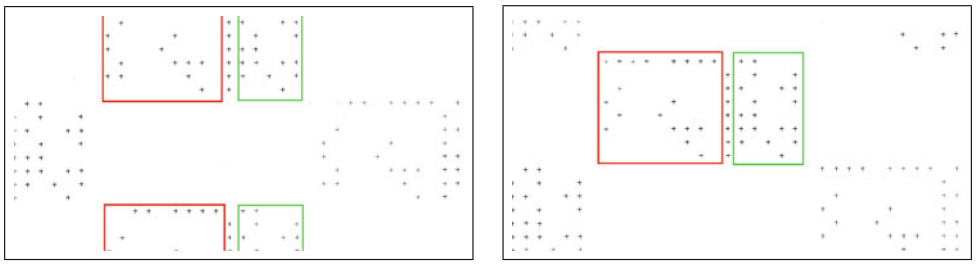

Fig. 14 Examples of differing patterns from the same Xerox printer. It can be seen that there is a considerable overlap in both patterns but some parts differ. The *red rectangle* shows the region where the time and date information is encoded. This region shows differences between the two patterns. The *green region* shows the serial number information (color figure online)

to decide if a dot is on or off, e.g. using a classification based on the computed frequencies.

Another issue is related to the matching of the fully populated search pattern; missing dots in the image at the border of the base pattern may lead to wrongly matched search pattern, which in consequence will lead to erroneous frequency counts for the base pattern dots.

8 Conclusion

In this paper, we presented considerable extension of our previous work on CPS code classification. The presented methods allow automatic comparison and decoding of CPS codes. This can be effectively used for authenticating printouts by identifying the source of the document. For evaluation purposes, the MIC dataset has been generated and made publicly available. It consists of sample sets of printouts of the EFF sample documents. The accuracy for pattern classification is shown to be up to 93 %. For CPS comparison an accuracy of 91.3 % is obtained. The decoding resulted in 98.3 % of the cases in a meaningful result.

Despite the advances of this work, unanswered questions about the CPS codes remain; on the one hand, it would be important to know the reason for the generation of the sparse patterns. On the other hand, evaluation would benefit if also the decoding of the patterns other than the

Table 5 Results of decoding the Xerox-type patterns

GT serial/type	Sam.	Img	Serial	Date	Time
D5W0012766	0004	0001	127666	00.00.00	00.00
Epson C4000 Aculaser		–	127666	00.00.00	00.00
		0009	127666	00.00.00	00.00
VF6004222	0015	0001	42222	00.00.00	00.00
XeroxPhaser 790		–	42222	00.00.00	00.00
		0009	42222	00.00.00	00.00
207768	0018	0001	207768	18.10.05	10:54
XeroxDocuColor 1632		0002	207768	18.10.05	11:04
		0003	207768	18.10.05	11:17
		0004	207768	18.10.05	11:46
		0005	207768	18.10.05	12:03
		0006	207768	18.10.05	11:49
		0007	207768	18.10.05	12:08
		0008	207768	18.10.05	12:24
		0009	207768	18.10.05	12:15
FZ20000126	0021	0001	126	00.00.00	00.00
EpsonC3000 Aculaser		–	126	00.00.00	00.00
		0009	126	00.00.00	00.00
CN-0PF019-73240-6CF-4002	0034	0001	1114002	32.00.00	64.00
Dell 3110CN		–	1114002	32.00.00	64.00
		0009	1114002	32.00.00	64.00
NA	0039	0002	29246	20.06.05	08:41
XeroxDocuColor 6060		0003	29246	20.06.05	08:41
		0004	29246	20.06.05	08:40
		0005	29246	20.06.05	08:40
		0006	29246	20.06.05	08:39
		0007	29246	20.06.05	08:39
		0008	29246	20.06.05	08:38
		0009	29246	20.06.05	08:37
NA	0040	0002	324928	24.06.05	18:44
XeroxDocuColor 2045		–	324928	24.06.05	18:44
		0009	324928	24.06.05	18:44
NA, Xerox DocuColor 12	0041	**All**	Sparse	Sparse	Sparse
CN-0J6508-71971-49I-B055	0044	0001	1322	00.00.00	00.00
Dell 5100CN		–	1322	00.00.00	00.00
		0009	1322	00.00.00	00.00
F2PZ119714	0053	0001	119714	00.00.00	00.00
EpsonC1100 Aculaser		–	119714	00.00.00	00.00
		0009	119714	00.00.00	00.00
NA	0072	0002	1071	25.06.05	10:38
XeroxDocuColor12		–	1071	25.06.05	10:38
		0009	1071	25.06.05	10:38
RLU000972	0108	0001	972	27.12.04	21:39
XeroxWorkcentre M24		0002	972	27.12.04	21:32
		0003	972	27.12.04	21:33
		0004	05	80.00.04	64.55
		0005	972	27.12.04	05:36
		0006	972	27.12.04	21:36

Table 5 continued

GT serial/type	Sam.	Img	Serial	Date	Time
		0007	972	27.12.04	21:37
		0008	972	27.12.04	21:38
		0009	972	27.12.04	21:38
3116491345	0109[a]	0001	649134	29.07.05	12:32
Xerox Workcentre Pro C2636		0002	649134	29.07.05	13:29
		0003	649134	29.07.05	13:30
		0004	649134	29.07.05	13:29
		0005	649134	29.07.05	13:31
		0006	649134	29.07.05	13:00
		0007	649134	29.07.05	13:00
		0008	9034	29.05.05	13:00
		0009	649134	29.07.05	13:00
NA	0115	0001	19178	00.00.00	00.00
DellLaser Printer 5100CN		–	19178	00.00.00	00.00
		0009	19178	00.00.00	00.00
NA	0115	0001	34880	00.00.00	00.00
DellLaser Printer 5100CN		–	34880	00.00.00	00.00
		0009	34880	00.00.00	00.00

The three rightmost columns show the extracted serial number, date and time. It can be seen that not all Xerox-type pattern actually contain date and time information. Also, different printer manufacturers use the same pattern type but seem to encode different information, as can be seen on the Dell 3110CN

The image number in bold indicate the cases for which the decoding did not provide the expected result

[a] The decoding method did not recognize the orientation of the pattern correctly due to a different scheme of the constant pattern parts. Therefore, the orientation was manually corrected as the evaluation focuses on the correct detection of the base pattern and not on the correctness of the decoding scheme

Xerox type would be known. To achieve these goals, more community effort is needed.

References

1. Ali GN, Chiang P-J, Mikkilineni AK, Allebach JP, Chiu GTC, Delp EJ (2005) Intrinsic and extrinsic signatures for information hiding and secure printing with electrophotographic devices. In: Proceedings of the international conference on digital printing technologies, New Orleans, September, pp 511–515
2. Amidror I (2002) A new print-based security strategy for the protection of valuable documents and products using moire intensity profiles. In: Proceedings of SPIE optical security and counterfeit deterrence techniques IV [1], pp 89–100
3. Breuel TM (2001) A practical, globally optimal algorithm for geometric matching under uncertainty. Electron Notes Theor Comput Sci 46:1–15
4. Breuel TM (2003) Implementation techniques for geometric branch-and-bound matching methods. Comput Vis Image Underst 90(3):258–294
5. Ball GR, Stittmeyer R, Srihari SN (2010) Writer verification in historical documents. In: Proceedings of SPIE document recognition and retrieval XVII, vol 7543, San Jose, January, pp 1–8
6. Breuel TM (2008) Binary morphology and related operations on run-length representations. In: Proceedings of the 3rd international conference on computer vision theory and applications, Funchal, January, pp 159–166
7. Chen S, Srihari S (2006) A new off-line signature verification method based on graph. In: Proceedings of the 18th international conference on pattern recognition, Hong Kong, August, pp 869–872
8. Choi J-H, Im D-H, Lee H-Y, Oh J-T, Ryu J-H, Lee H-K (2009) Color laser printer identification by analyzing statistical features on discrete wavelet transform. In: Proceedings of the 16th international conference on image processing, Cairo, November, pp 1505–1508
9. Electronic Frontier Foundation (2010) Docucolor tracking dot decoding guide. http://w2.eff.org/Privacy/printers/docucolor/ (accessed on 14.05.2010)
10. Hails J (2004) Criminal evidence. Thomson, Learning
11. Hampp NA, Neebe M, Juchem T, Wolperdinger M, Geiger M, Schmuck A (2004) Multifunctional optical security features based on bacteriorhodopsin. In: Proceedings of SPIE optical security and counterfeit deterrence techniques V [2], pp 117–124
12. Jiang W, Ho ATS, Treharne H, Shi YQ (2010) A novel multi-size block Benford's law scheme for printer identification, Shanghai, September, pp 643–652
13. Khanna N, Mikkilineni AK, Chiu GTC, Allebach JP, Delp EJ (2008) Survey of scanner and printer forensics at Purdue university. In: Proceedings of the 2nd international workshop on computational forensics [3], pp 22–34
14. Mikkilineni AK, Chiang P-J, Ali GN, Chiu GTC, Allebach JP, Delp EJ (2005) Printer identification based on graylevel co-occurrence features for security and forensic applications. In: Proceedings of SPIE security, steganography, and watermarking of multimedia contents VII, vol 5681, San Jose, February, pp 430–440

15. MIT Media Lab (2009) Initiative to stop the use of tracking dots. http://www.seeingyellow.com (accessed on 18.12.2009)
16. Otsu N (1979) A threshold selection method from gray-level histograms. IEEE Trans Syst Man Cybern 9(1):62–66
17. Pu D, Ball GR, Srihari SN (2009) A machine learning approach to off-line signature verification using Bayesian inference. In: Proceedings of the 3rd international workshop on computational forensics, Lecture notes in computer science, vol 5718, The Hague, August, pp 125–136
18. Sauvola J, Pietikainen M (2000) Adaptive document image binarization. Pattern Recogn 33(2):225–236
19. Schomaker L, Bulacu M (2004) Automatic writer identification using connected-component contours and edge-based features of uppercase western script. IEEE Trans Pattern Anal Mach Intell 26(6):787–798
20. Shannon CE (1948) A mathematical theory of communication. Bell Syst Tech J 27:379–423, 623–656
21. Schomaker L, Bulacu M, Franke K (2004) Automatic writer identification using fragmented connected-component contours. In: Proceedings of the 9th international workshop on frontiers in handwriting recognition, Tokyo, October, pp 185–190
22. Schreyer M (2009) Intelligent printing technique recognition and photocopy detection for forensic document examination. In: Proceedings of Informatiktage, vol S-8, Bonn, pp 39–42
23. Schulze C, Schreyer M, Stahl A, Breuel TM (2008) Evaluation of graylevel-features for printing technique classification in high-throughput document management systems. In: Proceedings of the 2nd international workshop on computational forensics [3], pp 35–46
24. Schulze C, Schreyer M, Stahl A, Breuel TM (2009). Using DCT features for printing technique and copy detection. In: Proceedings of the 5th international conference on digital forensics, Orlando, January, pp 95–106
25. Shafait F, Keysers D, Breuel TM (2008) Efficient implementation of local adaptive thresholding techniques using integral images. In: Proceedings of SPIE document recognition and retrieval XV, vol 6815, San Jose, January, pp 681510–681510
26. Smith PJ, O'Doherty P, Luna C, McCarthy S (2004) Commercial anticounterfeit products using machine vision. In: Proceedings of SPIE optical security and counterfeit deterrence techniques V [2], pp 237–243
27. Tweedy JS (2001) Class characteristics of counterfeit protection system codes of color laser copiers. J Am Soc of Quest Doc Exam 4(2):53–66
28. van Beusekom J, Schreyer M, Breuel TM (2010) Automatic counterfeit protection system code classification. In: Proceedings of SPIE media forensics and security XII, San Jose, January
29. van Beusekom J, Shafait F, Breuel TM (2010) Combined orientation and skew detection using geometric text-line modeling. Int J Doc Anal Recogn 13(2):79–92
30. van Renesse R (1995) Ordering the order, a survey of optical document security features. In: Proceedings of SPIE conference on practical holography IX, San Jose, February, pp 268–275
31. van Renesse R (1997) Paper based document security—a review. In: European conference on security and detection, London, April, pp 75–80
32. van Renesse R (2002) Hidden and scambled images—a review. In: Proceedings of SPIE optical security and counterfeit deterrence techniques IV [1], pp 333–348
33. van Renesse R (2006) Protection of high security documents—developments in holography to secure the future market and serve the public. In: Proceedings of Holo-Pack.Holo-Print, Vienna, November
34. van Renesse RL (2002)Proceedings of SPIE optical security and counterfeit deterrence techniques IV, vol 4677, San Jose, January
35. van Renesse RL (2004) Proceedings of SPIE optical security and counterfeit deterrence techniques V, vol 5310, San Jose, January
36. van Renesse RL (2008) Proceedings of the 2nd international workshop on computational forensics, Lecture notes in computer science, vol 5158, Washington, August